Oxygen isotopes in tree rings are a good proxy for Amazon precipitation and El Niño-Southern Oscillation variability

Roel J. W. Brienen[a,b,1], Gerd Helle[c], Thijs L. Pons[d], Jean-Loup Guyot[e], and Manuel Gloor[a]

[a]Department of Ecology and Global Change, School of Geography, University of Leeds, Leeds LS2 9JT, United Kingdom; [b]Department of Plant Ecology and Biodiversity and [d]Department of Plant Ecophysiology, Institute of Environmental Biology, Utrecht University, 3508 TB Utrecht, The Netherlands; [c]Helmholtz Centre Potsdam, German Research Centre for Geosciences, Department of Climate Dynamics and Landscape Evolution, Telegrafenberg, 14473 Potsdam, Germany; and [e]Institut de Recherche pour le Développement, Lima, Peru

Edited by Robert E. Dickinson, University of Texas at Austin, Austin, TX, and approved September 10, 2012 (received for review April 26, 2012)

We present a unique proxy for the reconstruction of variation in precipitation over the Amazon: oxygen isotope ratios in annual rings in tropical cedar (*Cedrela odorata*). A century-long record from northern Bolivia shows that tree rings preserve the signal of oxygen isotopes in precipitation during the wet season, with weaker influences of temperature and vapor pressure. Tree ring $\delta^{18}O$ correlates strongly with $\delta^{18}O$ in precipitation from distant stations in the center and west of the basin, and with Andean ice core $\delta^{18}O$ showing that the signal is coherent over large areas. The signal correlates most strongly with basin-wide precipitation and Amazon river discharge. We attribute the strength of this (negative) correlation mainly to the cumulative rainout processes of oxygen isotopes (Rayleigh distillation) in air parcels during westward transport across the basin. We further find a clear signature of the El Niño-Southern Oscillation (ENSO) in the record, with strong ENSO influences over recent decades, but weaker influence from 1925 to 1975 indicating decadal scale variation in the controls on the hydrological cycle. The record exhibits a significant increase in $\delta^{18}O$ over the 20th century consistent with increases in Andean $\delta^{18}O$ ice core and lake records, which we tentatively attribute to increased water vapor transport into the basin. Taking these data together, our record reveals a fresh path to diagnose and improve our understanding of variation and trends of the hydrological cycle of the world's largest river catchment.

climate change | dendrochronology | plant physiology

The Amazon basin is a major center of atmospheric convection and precipitation (1), and at the same time the world's largest drainage basin. The Amazon's river discharge accounts for ~17% of the annual global discharge to the oceans (2); its hydrological cycle is tightly linked with the carbon cycle of the Amazon rainforest (3), which itself is one of the largest terrestrial biomass carbon pools. Changes in the hydrological cycle of the Amazon may therefore significantly affect atmospheric dynamics and global climate by changing atmospheric CO_2 concentration. Two particularly severe droughts occurred within the last decade (4), and long-term river records of the Amazon show a steady increase in discharge over the last century (5), indicating that the system may start to undergo some changes. It has been suggested that these changes are a result of anthropogenic warming, but they may also be part of longer-term, natural climatic variability. To clarify such a globally important issue, long-term, accurate records of the hydrological cycle of the Amazon basin are needed. However, meteorological data are only reliable for the last 50–60 y (6), and annually resolved long-term proxies for the hydrological cycle from within the Amazon basin itself are very scarce (7).

A commonly used diagnostic for strength and functioning of the water cycle is the isotopic composition of precipitation. Although variation of oxygen isotope ratios in precipitation in temperate to arctic regions is determined among other factors by the condensation temperature (8), the dominant contributing factors over tropical land are rather Rayleigh distillation [because of changes in the isotopic water vapor content of air when traveling inland caused by precipitation (9, 10)], recycling of rainwater (11), and local precipitation intensity (cf. "amount effect," refs. 8, 12, and 13). Observations of the isotopic composition of meteoric precipitation over South America show that isotopic composition is indeed closely associated with the amount of precipitation along the air parcel path (10), which suggests that oxygen isotopes in precipitation are predominantly a proxy for the large-scale atmospheric component of the basin-wide hydrological cycle (9, 14). However, the interpretation of results from paleoclimatic studies of oxygen isotopes in ice cores (15–17), lake sediments (18), and speleothems (19, 20) remains disputed, and proxies have been interpreted variously as indicators of temperature (17), basin-wide rainfall (18–21), or a combination of both (22). Despite numerous oxygen paleorecords from the Andes, there are no such proxies from within the Amazon basin itself.

A promising new method for the reconstruction of Amazon precipitation is oxygen isotopes in tree-ring cellulose ($\delta^{18}O_{tr}$). However, the conditions and degree to which tropical tree rings record variation in oxygen isotopes in precipitation, and thus indeed contain information about the hydrological cycle, remains poorly known (23). Oxygen isotopic values in tree rings are believed to mainly reflect isotopic composition of soil water and plant physiological effects, like leaf-water enrichment and oxygen isotope exchange reactions of photosynthates with water (24, 25). The degree to which these factors influence the signal of oxygen isotopes in tree rings may vary between sites and species (24). In the tropics, the number of oxygen isotope studies is small, although recently has been increasing. The few studies undertaken so far show that oxygen isotope signals in wood of lowland tropical trees are often dominated by a negative influence of precipitation amount (7, 23, 26), but correlations are often weak (7). Positive correlations with rainfall amount have also been found (26). Still, the number of long tree-ring isotope chronologies is small, and the factors controlling variation in tree-ring oxygen isotope ratios in lowland tropics remain poorly understood.

In this study, a unique annually resolved isotope record from well-dated tree rings of *Cedrela odorata* from the Amazon basin is presented. These trees are a prime candidate to record variation in precipitation $\delta^{18}O$ because *C. odorata* has a relatively superficial root-system and relies strongly on water from the topsoil layer (27). We first analyze the relation between variation in tree-ring oxygen isotopes and isotopic composition of soil water using records of oxygen isotopes in meteoric rainwater and from Andean glaciers. We then quantify the effect of climate on interannual variation in tree-ring oxygen isotopes by relating our records to local and basin-wide climate variables and to discharge data of the Amazon River

Author contributions: R.J.W.B., G.H., T.L.P., J.-L.G., and M.G. designed research; R.J.W.B. and G.H. performed research; R.J.W.B., G.H., and M.G. analyzed data; and R.J.W.B. and M.G. wrote the paper.

The authors declare no conflict of interest.

This article is a PNAS Direct Submission.

Freely available online through the PNAS open access option.

[1]To whom correspondence should be addressed. E-mail: r.brienen@leeds.ac.uk.

This article contains supporting information online at www.pnas.org/lookup/suppl/doi:10.1073/pnas.1205977109/-/DCSupplemental.

at Obidos. Finally, we explore the influence of the associated large-scale climate drivers for the Amazon [e.g., influence of El Niños and Atlantic sea-surface temperatures (SSTs)], and discuss the wider importance of our findings.

Results and Discussion

What Controls Oxygen Isotopes in *Cedrela* Tree Rings? As tree roots take-up soil water without fractionation of the heavier $H_2{}^{18}O$ (24, 25), at least part of the isotopic signature in tree rings should reflect variation in precipitation $\delta^{18}O$. To test this hypothesis, we correlated $\delta^{18}O_{tr}$ with isotopic ratios in meteoric precipitation (data; Global Network of Isotopes in Precipitation; see *SI Appendix*), which shows indeed significant relations with various stations across the Amazon Basin (Fig. 1). Among the station records, the correlation is strongest with annual values of oxygen isotopes in precipitation ($\delta^{18}O_{prec}$) from Manaus ($r = 0.86$, $n = 15$). Generally variation in $\delta^{18}O_{tr}$ correlated most strongly with $\delta^{18}O$ in precipitation during the wet season (December–May), which corresponds to the main period of growth for this drought-deciduous species (*SI Appendix*, Fig. S3) (28).

Additional support for a dominant influence of the soil-water signal on $\delta^{18}O_{tr}$ comes from a comparison of the tree-ring record with $\delta^{18}O$ from Andean glaciers (15, 17), which have primarily been interpreted as indicators of $\delta^{18}O$ in atmospheric water vapor from the Amazon basin (21). We find a relatively strong correlation with the Quelccaya and Huascarán ice core records (Quelccaya, 1963–1984, $r = 0.77$; Huascaran, 1963–1992, $r = 0.68$), and somewhat lower correlation with the Sajama ice core record (1963–1997, $r = 0.44$).

Plant physiological models using $\delta^{18}O$ predict that tree-ring cellulose is not only influenced by soil water but also by evaporative enrichment of transpiring leaves (25). To explore to what degree the interannual variation in $\delta^{18}O$ in *Cedrela* tree rings contains such signals, we related $\delta^{18}O_{tr}$ to locally recorded climate variables and found statistically significant relationships of local precipitation, temperature, and vapor pressure (*SI Appendix*, Table S2). The effect of interannual variation in isotopic composition of precipitation is bigger however (correlations in Fig. 1). Although we do not have additional ecophysiological data (e.g., daily leaf temperature and stomatal conductance) to detect the plant physiological influences, overall results indicate that plant physiological controls are relatively small (see *SI Appendix* for further details). This finding differs from Kahmen et al. (29), showing that leaf-to-air vapor pressure was the main control of plant $\delta^{18}O$ along an altitudinal gradient. For our species at this site, the dominant control of interannual variation in $\delta^{18}O_{tr}$ seems to be interannual variation in the isotopic composition of meteoric precipitation ($\delta^{18}O_{prec}$).

Climatic Signals in Tree-Ring Oxygen Isotopes at Interannual to Decadal Time Scales. Our record provides an annually resolved reconstruction of oxygen isotopes for the last 100 y, and thus allows for an analysis of climatic controls on oxygen isotopes in tree rings, and thereby precipitation over the Amazon. We find that the amount of precipitation over the entire Amazon basin has the strongest correlations with $\delta^{18}O_{tr}$ (Fig. 2). There are also significant correlations with temperature and vapor pressure, but these are weaker and decrease or disappear entirely when controlling for the influence of (basin-wide, wet season) precipitation (*SI Appendix*, Table S3). This finding suggests that the amount of basin-wide precipitation during the wet season exerts the strongest influence on $\delta^{18}O_{tr}$. Consequently, we also find a remarkably strong correlation with the Amazon discharge measured at Obidos at interannual to decadal scales (Fig. 2). The correlations with river discharge, calculated for different time periods over the 20th century, remained relatively high for the entire record (varying between –0.80 over recent decades to –0.53 at the start of the century) (*SI Appendix*, Table S4), but the strength of the correlation with the precipitation record decreased more strongly (i.e., from –0.85 to –0.33) (*SI Appendix*, Table S3). This finding indicates that the influence of the amount of basin-wide precipitation on oxygen isotopic composition is stationary over longer time scales and that decreasing correlations with precipitation data further back in time are likely because of poor quality and low spatial resolution of the precipitation dataset at the start of the century (6). Known extreme dry years are clearly visible in the oxygen isotope record (Fig. 2). Notably, the driest year over the last

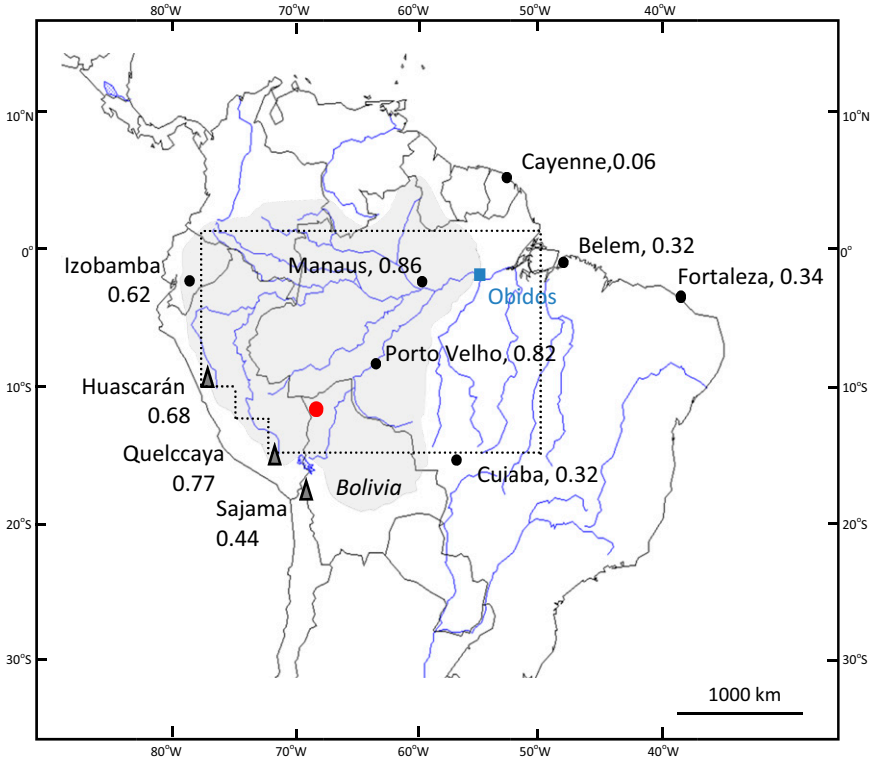

Fig. 1. Map of the Amazon indicating the study site (red dot), stations with records of $\delta^{18}O$ in meteoric precipitation (black dots), Andean glaciers with records of $\delta^{18}O$ (triangles), and the location of the Amazon River discharge records at Obidos (blue square). The shaded area shows the area of the catchment of the Amazon River that discharges at Obidos, an area encompassing 77% of the entire basin, or 4.68 million km^2 (5). The broken line indicates area from which climate data for the whole basin were extracted. Values next to the station names and glaciers indicate the correlation coefficients between $\delta^{18}O_{tr}$ and $\delta^{18}O$ measured in precipitation or ice cores at those sites. For details on data sources for $\delta^{18}O$ records, see *SI Appendix*.

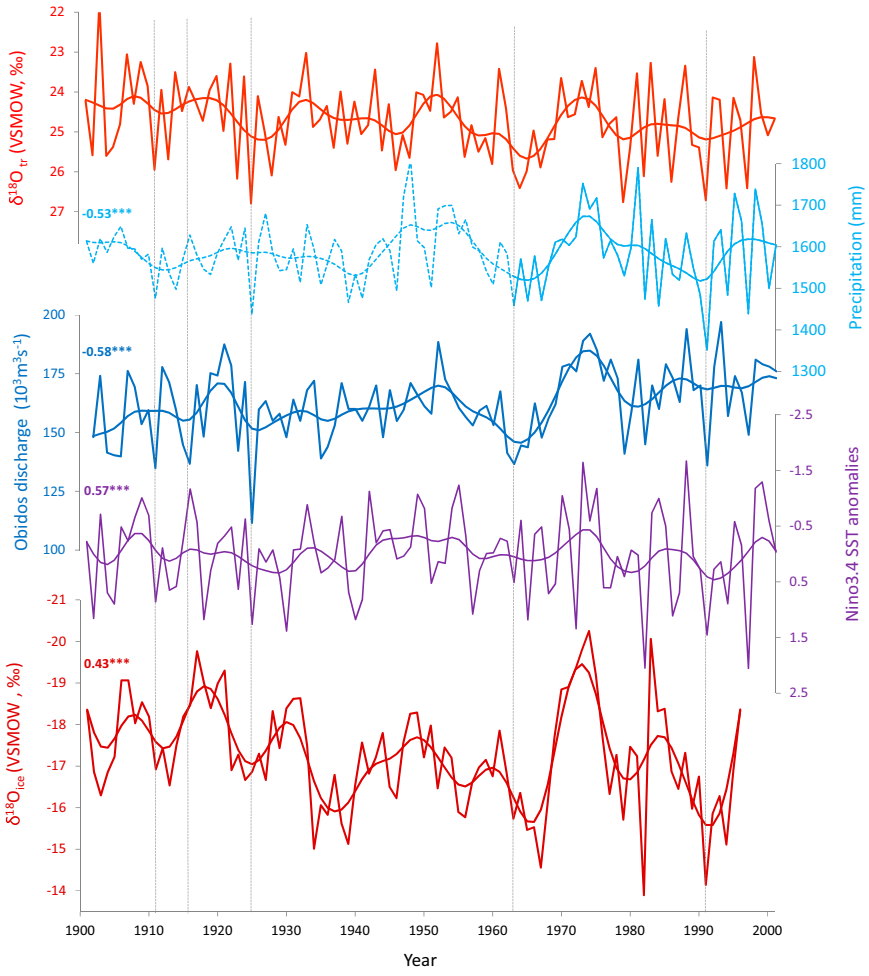

Fig. 2. Time series of $\delta^{18}O$ in tree ring cellulose of *C. odorata* (Purissima, Bolivia), wet season precipitation over the Amazon basin (2.5°N–15.0°S, 50°–77.5°W, Climatic Research Unit TS3.1, broken part of line indicate less reliable records < 1963), Obidos river discharge (5), wet season Niño3.4 SST anomalies, and mean ice core $\delta^{18}O$ [i.e., arithmetic mean of Huascaran, Quelccaya (17),and Sajama glaciers (15)]. Broken vertical lines indicate the 5 y (1925–1926, 1911–1912, 1991–1992, 1963–1964, and 1916–1917) with the lowest Obidos river discharge of the 1901–2001 period, a good indicator of severe droughts over the Amazon Basin. A low-pass, Butterworth filter was applied to each of these time series to visualize decadal scale variation (see *Methods*). Values indicate the Pearson correlation coefficients between the $\delta^{18}O_{tr}$ and other records for the full period shown (for all $P < 0.001$). Note that the *y* axis for the $\delta^{18}O$ series and the Niño3.4 SST are reversed.

century, the El Niño-Southern Oscillation (ENSO) related drought of 1925–1926 (30), also shows the highest excursion in the entire $\delta^{18}O_{tr}$ record. The finding that $\delta^{18}O_{tr}$ is primarily related to interannual changes in wet season precipitation, agrees also with findings in tree rings from Costa Rican cloud forests (31) and northern Laos (32).

The observed influence of precipitation on the oxygen signal is in line with climate-model results (9, 14), and with observations on the relationship between $\delta^{18}O_{prec}$ and (amount of) precipitation in the Amazon (10, 14). Our results thus support the idea that glacier and other oxygen isotope records in the Andes or subtropical Brazil (33) should primarily be interpreted as a precipitation record (18, 20, 21), and are much less a proxy for temperature. The strong similarity between our record and those from Andean ice cores (Fig. 2) shows that a large portion of variation in ice core $\delta^{18}O$ can be attributed to variation in $\delta^{18}O$ from the Amazon basin, but with greater variation in the Andean ice cores because of orographic lift of air over the Andes, resulting in further rainout processes (17, 34). Given the similar controls of these records, it is thus tempting to argue that the observed low isotope values in Andean ice cores during the last glacial maximum (LGM, ca. 18–21 ka ago) indicate that the Amazon was wetter during the LGM than it is today. This finding would be consistent with independent inferences of wetter conditions during the LGM based on lake records in the Altiplano (35), but inconsistent with pollen evidence (36) or Amazon river outflow reconstructions based on a marine foraminifera $\delta^{18}O$ record (37), indicating that the Amazon was drier than today. A scenario of a drier Amazon seems difficult to reconcile with wetter Andes indicated by ice core records during the LGM. However, factors other than precipitation may play a role for $\delta^{18}O$ in precipitation. For example, a greater fraction of run-off from total water vapor available within the basin, because of changes in forest type or larger extent of savannah during the LGM (36), leads to decreases in $\delta^{18}O$ at the end of the water vapor trajectory (22). Similarly, large-scale circulation changes associated, e.g., with shifts in orbital forcing may have changed the moisture transport trajectory to the Andes (33).

Large-Scale Drivers of Interannual to Decadal Variation in Tree-Ring Oxygen Isotopes. A major driver behind interannual variation in precipitation in the tropics and the Amazon basin is the ENSO (1, 3, 38, 39). El Niño-years are associated with decreased convection over the Amazon basin (3). We find indeed a positive correlation between $\delta^{18}O_{tr}$ and SST in the central equatorial pacific (the Niño3.4 region) (Figs. 2 and 3). This Pacific influence is strongest during the austral summer (i.e., peak of the rainy season) (*SI Appendix*, Table S5). Besides this well-known Pacific influence, precipitation over the Amazon is also influenced by tropical Atlantic SST, but mainly during the dry season (38). This finding probably explains the lack of high correlations between $\delta^{18}O_{tr}$ and Atlantic SSTs at interannual scales, as $\delta^{18}O_{tr}$ records $\delta^{18}O_{prec}$ during the rainy season and not the dry season (*SI Appendix*, Fig. S3). However, tropical north Atlantic SST anomalies do show strong parallels with our record at decadal and longer time scales, both exhibiting positive trends over time (*SI Appendix*, Fig. S6).

Interestingly, although the effect of ENSO on precipitation (amount) at the study site itself is relatively weak (*SI Appendix*, Table S1), the correlation of $\delta^{18}O_{tr}$ with ENSO is strong. These results and observations of ENSO signals in Andean ice core records (16) indicate that it is the large-scale atmospheric circulation that controls

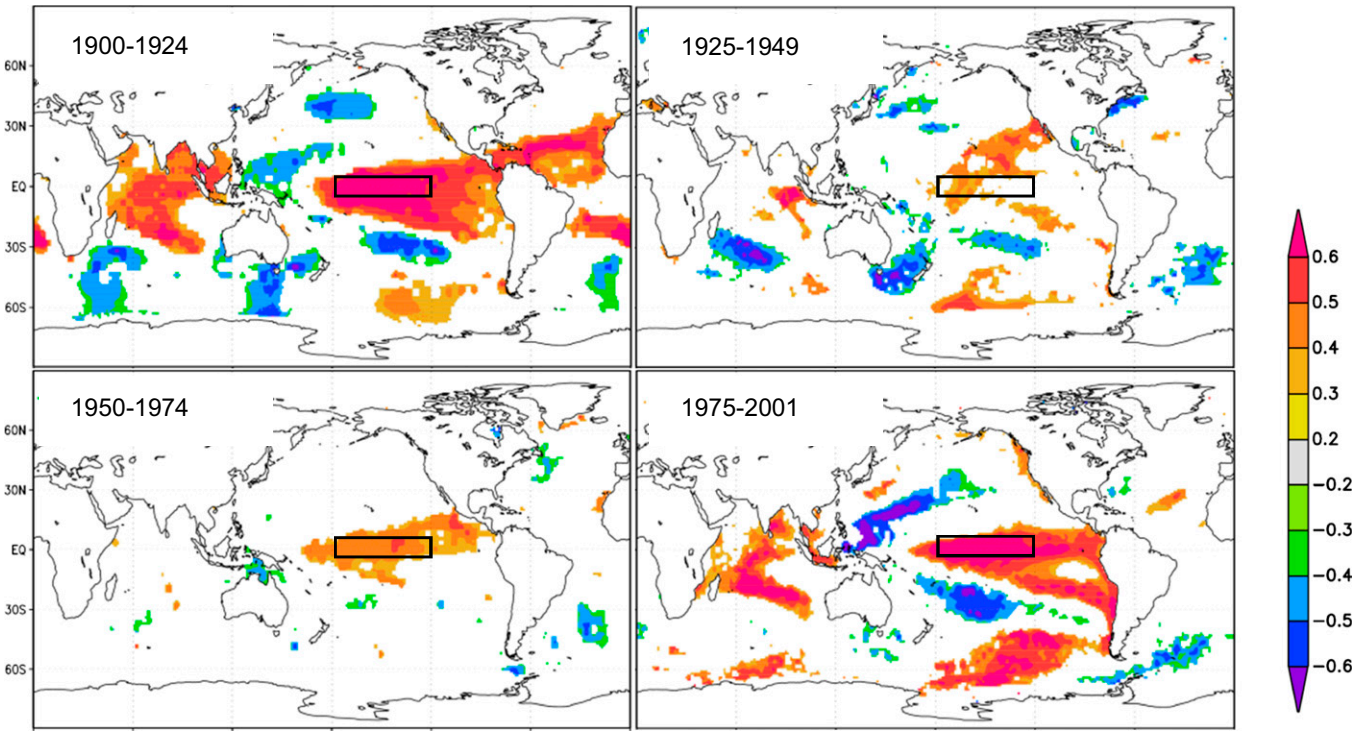

Fig. 3. Correlations between $\delta^{18}O_{tr}$ and gridded global SSTs (data:HadISST1) during the wet season (i.e., October to April) for different time periods of the last century. Values on the color scale correspond to correlation coefficients ($P < 0.01$). The square in the Pacific Ocean indicates the Niño3.4 region (5°S–5°N, 120°W–170°W).

the $\delta^{18}O$ signal in the Amazon basin, and not a local amount effect (i.e., a negative correlation between the rate of precipitation and $\delta^{18}O$ in local precipitation) (12, 13), consistent with model predictions (14). Similar controls of ENSO on the isotopic signature in tree rings were observed in Costa Rica (40) and Asia (32, 41), and negative correlations were observed along the west coast of Peru, where warm-phase ENSO events result in increased precipitation and thus negative excursions in $\delta^{18}O$ (23). These tree-ring isotope studies show that ENSO affects interannual variation in plant $\delta^{18}O$ over large areas in the tropics. As the tropics are also regions with very high net primary productivity, this pan-tropically coherent ENSO signal in plant water $\delta^{18}O$ is passed on to oxygen isotope ratios in atmospheric CO_2 through biosphere-atmosphere gas exchange, and leads to higher $\delta^{18}O$ in atmospheric CO_2 several months after El Niño's occurred (42). In all, our results confirm the potential of tree ring $\delta^{18}O$ to elucidate historical influences of ENSO on precipitation in the tropics.

The influence of ENSO is not always equally dominant, showing a weaker influence on our isotope record during the middle of the century and stronger influence during the beginning and end of the last century (Fig. 3). The reduced influence of ENSO during the middle of the century coincides with periods of lower variance in the Southern Oscillation Index (the atmospheric branch of El Niño) (43), weaker correlations between ENSO and precipitation in the Amazon (1), and lower interannual variation in precipitation and Obidos records (5, 39) during 1920–1960. At decadal scales the oxygen isotope record also shows a big shift in the oxygen isotope record around the 1970s, probably related to an abrupt warming of the tropical Pacific and change in sign of the Pacific Decadal Oscillation (1).

Possible Mechanisms Underlying the Strong Precipitation Signal in $\delta^{18}O_{tr}$. It is quite remarkable that oxygen isotopes in tree rings of just eight trees from one single site are such a good proxy of precipitation in the whole Amazon catchment basin of approximately 5 million km^2. What are the underlying mechanisms for this strong coherence? Variation in the isotope signal in precipitation is a mixture of local effects (e.g., local precipitation intensity) and large-scale influences (e.g., changes in isotopic signature during water vapor transport into the basin). The lack of strong correlations of $\delta^{18}O_{tr}$ with local climate records and the strong decrease in correlations after controlling for the effect of basin-wide precipitation (*SI Appendix*, Table S3), suggest that the isotopic signature in precipitation at our site reflects primarily what happens during water-vapor transport to the site rather than local precipitation amount. During air-parcel transport, two processes affect the isotopic composition of its water-vapor content. First, heavy isotopes tend to condense more readily, and thus water vapor gets gradually more depleted during transport over land [i.e., water vapor loses relatively more of the heavier isotopes ($H_2{}^{18}O$) because of the classic Rayleigh distillation (8)]. The degree of total "rainout" of heavy isotopes depends on the fraction of water that is removed from a particular air parcel, and is thus generally larger during years with high amounts of precipitation along the air-parcel trajectory than during years with low precipitation. Therefore, this mechanism leads to more depleted water vapor (more negative $\delta^{18}O$) at the end of the trajectory during wet years compared with dry years. A second process that may affect the isotopic composition of water vapor is recycling of rainwater by vegetation (11). Tropical rainforest transpires large amounts of water through transpiration by stomata and direct evaporation of water from leaf surfaces during the day; it is estimated that up to 60% of the yearly precipitation is returned into the atmosphere, much of which will eventually condense again (11, 44). As evapotranspiration is approximately a nonfractionating process with respect to oxygen isotopes (i.e., water vapor leaving the leaf has the same isotopic signature as stem water), once a transpirational steady-state has been reached in the leaf (45), large amounts of water vapor with an isotopic signal similar to that of soil water are returned to the atmosphere. The isotopic signature of this recycled water from vegetation into the atmosphere will be relatively lighter (i.e., has a lower $\delta^{18}O$) during years with high precipitation, as the precipitation from which the vapor originates is lighter because of the amount effect (12, 13). Continuous recycling of water along the trajectory thus adds more and more water vapor to the airstream traveling westward, which carries an isotopic "memory" of the local amount effect. Because

recycling may contribute to more than half of the precipitation in the western part of the basin (estimates vary between 50% and 88%) (46, 47), isotopic signatures in these parts of the Amazon are therefore also expected to be partly a reflection of the accumulated local amount effects. We expect that these two mechanisms will enhance the differences in the isotopic signal between dry and wet years along the water-vapor trajectory, and thus exacerbate difference in isotopic signal in the western and eastern part of the basin.

We do find some evidence for this in our data as our tree-ring record correlated better with observational data of $\delta^{18}O$ in the western and center of the Amazon basin and with Andean ice cores, than with $\delta^{18}O_{prec}$ records at the east (see, for example, correlation coefficients in Fig. 1). This finding seems to confirm that the isotopic imprint in water vapor indeed changes from east to west. The specific location of our study site means that each air parcel has traveled at least 2,500 km from its origin in the tropical north Atlantic to the southwest of the basin (*SI Appendix*, Fig. S5), which probably played a major role in making the signal so particularly strong.

Long-Term Trends in Tree-Ring Oxygen Isotopes. In contrast to the tight correlation at interannual time scales, we find that the trends of $\delta^{18}O_{tr}$ and Amazon precipitation diverge over longer time scales. Obidos river discharge (5) and the Global Precipitation Climatology Centre precipitation dataset both show increases over the last century, but not Climatic Research Unit precipitation (*SI Appendix*, Fig. S7). If the $\delta^{18}O_{tr}$ records would have followed directly this river discharge and precipitation trend over the last century, we would expect a decrease in long-term $\delta^{18}O_{tr}$, but instead we find a significant increase of 0.5‰ in $\delta^{18}O_{tr}$ over the last century (*SI Appendix*, Fig. S2). A comparison with Andean ice core records (Fig. 2) (48), Andean lake sediments (18), and speleothems at the Andean foothills (20) reveal parallel increases in $\delta^{18}O$ since approximately 1850. We interpret this long-term increase in $\delta^{18}O_{tr}$ therefore as a result of increasing $\delta^{18}O$ in precipitation over the basin rather than because of plant physiological changes during ontogeny. Studies that specifically looked at physiological $\delta^{18}O$ trends in tree rings found a negative trend with age (49). Although this study was performed in a substantial different climatic zone, we argue that a strong ontogenetic (i.e., age- or size-related) -positive $\delta^{18}O$ trend is not very likely.

Previous studies have interpreted these recent increases in $\delta^{18}O$ differently. Thompson et al. (48) attributed the increases since 1850 to increases in air temperature, in line with interpretation of mid and high latitude $\delta^{18}O_{prec}$ data (50). Although the magnitude of increases in temperature over the Amazon basin (0.77 °C over 100 y) may explain the increase of 0.5‰ in our record, support for a temperature effect at tropical latitudes is scarce. In contrast, Bird et al. (18) explain recent increases in their lake record as an indication of a general weakening of South American wet season precipitation, but such a weakening of South American wet season precipitation is at odds with the observed (upward) trends in Obidos river discharge and precipitation over the last century. We briefly explore other mechanisms that may explain these long-term trends. One possible mechanism is related to a change in the water balance of the basin, such as changes in the net amount of water vapor transported into the basin. The observed increases in river run-off and satellite observations on water-vapor transport (51) indicate that water import into the basin may have increased. If such increases in influx of water vapor exceed the increase in rainout and loss via river run-off, the isotope ratios would increase. This is because for this scenario a lower fraction of the total water vapor traveling into the basin is rained out before reaching our site, and thus water vapor export out of the basin would have to increase as well. The strong, recent increases in summer precipitation and run-off in the La Plata basin (south west of Brazil) (52) indicates that export of water vapor toward the south of the Amazon Basin did indeed increase over the last decades (53). Other possible mechanisms that affect the isotope signal include changes in cloud cover and convection (54) and decreases in evapotranspiration rates because of increases in atmospheric CO_2 (55) and deforestation. Decreases in evapotranspiration do affect the isotope signal, but would rather lead to a decrease in $\delta^{18}O$ over time at the west-end of the basin (56), and thus the opposite of what we observe. Although, we are not yet in a position to explain the observed trend, our results show that the upward trend in $\delta^{18}O$ is not because of drying of the Amazon (18), and that a temperature effect (48) also seems unlikely.

Outlook. Our proxy record shows that $\delta^{18}O$ in the Amazon is predominantly governed by large-scale variation in precipitation, but the relative importance of the different mechanisms that influence the signal remain elusive. One way of improving our understanding is by expanding the spatial and temporal coverage of $\delta^{18}O$ in tree rings or other proxies within the Amazon. Although our $\delta^{18}O_{tr}$ record covered only 100–150 y, *Cedrela* can become substantially older (i.e., > 300 y old) (28) and has a large geographic distribution (i.e., from 25°N to 25°S). Comparison of long-term trends at different extremes, or across different gradients in the Amazon basin could potentially reveal important insights as to what drives the long-term trends. For example, differences in long-term $\delta^{18}O$ trends along an east-west gradient may be indicative of long-term changes in water recycling, but differences in the north-south gradients may indicate changes in meridional positioning of the Intertropical Convergence Zone. An extension of the record in time may significantly improve our understanding of drivers over longer time scales, and allow testing of whether extreme events, like the droughts in 2005 and 2010, are increasing over time and are related to natural cycles or linked to global warming.

The coherence over large spatial scales of the isotopic signal in precipitation allows also, in theory, for a precise cross-dating of chronologies over long distances. For example, the interannual variation in oxygen isotopes in our site was similar to that of stations as far as 1300–1500 km to the north east and west of the basin (Fig. 1). Thus, as long as the trees use precipitation water in a similar way as *Cedrela*, and do not excessively use deeper groundwater, our isotope chronology could help assist the development of oxygen isotope chronologies from other sites and species, allowing more extensive sampling of the basin's hydrological history in time and space. Advantages of tree ring-based proxies are that records do not need to be limited to the Andes or location of caves, and that the records provide a much better resolution than, for example, speleothems or valve records.

Conclusions

We demonstrated that oxygen isotope ratios in tree rings in tropical *Cedrela* accurately record the isotopic composition of meteoric precipitation during the wet season ($\delta^{18}O_{prec}$) and show only weak controls by plant physiology. Isotope ratios in tree rings provide a very strong proxy for annual to decadal scale variation in the amount of precipitation over the entire Amazon basin and for basin-wide river discharge, and are only weakly correlated with temperature, vapor pressure, or local precipitation. The record shows significant correlations with $\delta^{18}O$ in precipitation in the central and western Amazon and ice cores in the Andes, indicating that the interannual variation in $\delta^{18}O$ of precipitation contains a spatially coherent signal over large parts of the Basin, consistent with model predictions. The most dominant large-scale control of variation in tree ring $\delta^{18}O$ at interannual scales is the ENSO, with a particularly strong influence over recent decades and a weakened influence during the middle of the last century. At longer time scales, the tree-ring oxygen isotope series showed a significantly increasing trend. These trends were previously interpreted as being a result of global warming or drying of the basin, but the true cause remains disputed. Our study shows that tree-ring oxygen isotopes can be used as a tracer for changes in meteoric $\delta^{18}O$ and is thus a highly promising tool for detecting long-term changes in the hydrological cycle of the basin.

Methods

Complete discs were collected from the bases of approximately 60 logged trees of *C. odorata* from undisturbed tropical moist lowland forest from Purissima, northern Bolivia (11°24′S, 68°43′W) (Fig. 1) in October 2002. Tree rings were measured and successfully cross-dated (28). For this study, we selected eight large

trees (>60 cm in diameter) and isolated wood from each individual ring along a single radius using sharp knives and razor blades. Procedures for cellulose extraction and homogenization are described in the *SI Appendix*. The samples were weighed and packed into silver capsules, and pyrolized at 1.080 °C in an element analyzer (Carlo Erba) coupled to an isotope spectrometer (OPTIMA; Micromass). Values are expressed relative to V-SMOW and have an analytic precision of 0.3‰. In all analysis we used the arithmetic mean isotope ratios of the different trees ($\delta^{18}O_{tr}$). Details on the sources of climate, $\delta^{18}O_{prec}$ and $\delta^{18}O_{ice}$ records are provided in the *SI Appendix*.

ACKNOWLEDGMENTS. We thank Carmen Buerger and Peter van der Sleen for their help with cellulose extraction and isotope analysis; Stephen Arnold for running the back-trajectories; and Jeanette Pacajes for help with the export of samples. R.J.W.B. was supported by Dirección General de Asuntos del Personal Académico of the Universidad Nacional Autónoma de México, the Gordon and Betty Moore Foundation [Grant to Amazon Forest Inventory Network (RAINFOR)], and a Research Fellowship from the United Kingdom Natural Environment Research Council. M.G. was financially supported by Amazon Integrated Carbon Analysis (AMAZONICA) (Natural Environment Research Council).

1. Garreaud RD, Vuille M, Compagnucci R, Marengo J (2009) Present-day South American climate. *Palaeogeogr Palaeoclimatol Palaeoecol* 281(3-4):180–195.
2. Callede J, et al. (2010) The River Amazon water contribution to the Atlantic Ocean. *J Water Sci* 23(3):247–273.
3. Foley JA, Botta A, Coe MT, Costa MH (2002) El Nino-Southern Oscillation and the climate, ecosystems and rivers of Amazonia. *Global Biogeochem Cycles* 16(4):1132.
4. Marengo JA, Tomasella J, Alves LM, Soares WR, Rodriguez DA (2011) The drought of 2010 in the context of historical droughts in the Amazon region. *Geophys Res Lett* 38: L12703.
5. Callede J, et al. (2004) Evolution of the River Amazon's discharge at Obidos from 1903 to 1999. *Hydrol Sci J* 49(1):85–97.
6. Costa MH, Coe MT, Guyot JL (2009) Effects of climatic variability and deforestation on surface water regimes. In *Amazonia and Global Change*, eds. Keller M, Bustamante M, Gash J, Silva Dias P (American Geophysical Union, Washington, DC), Monograph 186, p 576.
7. Ballantyne AP, Baker PA, Chambers JQ, Villalba R, Argollo J (2011) Regional differences in South American monsoon precipitation inferred from the growth and isotopic composition of tropical trees. *Earth Interact* 15(5):1–35.
8. Dansgaard W (1964) Stable isotopes in precipitation. *Tellus* 16:436–463.
9. Sturm C, Hoffmann G, Langmann B (2007) Simulation of the stable water isotopes in precipitation over South America: Comparing regional to global circulation models. *J Clim* 20:3730–3750.
10. Villacís M, Vimeux F, Taupin JD (2008) Analysis of the climate controls on the isotopic composition of precipitation ($\delta^{18}O$) at Nuevo Rocafuerte, 74.5°W, 0.9°S, 250 m, Ecuador. *C R Geosci* 340(1):1–9.
11. Salati E, Dallolio A, Matsui E, Gat JR (1979) Recycling of water in the Amazon Basin—Isotopic study. *Water Resour Res* 15:1250–1258.
12. Risi C, Bony S, Vimeux F (2008) Influence of convective processes on the isotopic composition ($\delta^{18}O$ and δD) of precipitation and water vapor in the tropics: 2. Physical interpretation of the amount effect. *J Geophys Res* 113:D19306.
13. Lee J-E, Fung I (2008) "Amount effect" of water isotopes and quantitative analysis of post-condensation processes. *Hydrol Process* 22(1):1–8.
14. Vuille M, Werner M (2005) Stable isotopes in precipitation recording South American summer monsoon and ENSO variability: Observations and model results. *Clim Dyn* 25: 401–413.
15. Hardy DR, Vuille M, Bradley RS (2003) Variability of snow accumulation and isotopic composition on Nevado Sajama, Bolivia. *J Geophys Res* 108(D22):4693.
16. Bradley RS, Vuille M, Hardy D, Thompson LG (2003) Low latitude ice cores record Pacific sea surface temperatures. *Geophys Res Lett* 30(4):1174.
17. Thompson LG, Mosley-Thompson E, Henderson KA (2000) Ice-core palaeoclimate records in tropical South America since the Last Glacial Maximum. *J Quat Sci* 15: 377–394.
18. Bird BW, et al. (2011) A 2,300-year-long annually resolved record of the South American summer monsoon from the Peruvian Andes. *Proc Natl Acad Sci USA* 108: 8583–8588.
19. van Breukelen MR, Vonhof HB, Hellstrom JC, Wester WCG, Kroon D (2008) Fossil dripwater in stalagmites reveals Holocene temperature and rainfall variation in Amazonia. *Earth Planet Sci Lett* 275:54–60.
20. Reuter J, et al. (2009) A new perspective on the hydroclimate variability in northern South America during the Little Ice Age. *Geophys Res Lett* 36:L21706.
21. Hoffmann G, et al. (2003) Coherent isotope history of Andean ice cores over the last century. *Geophys Res Lett* 30:1179.
22. Pierrehumbert RT (1999) Huascaran $\delta^{18}O$ as an indicator of tropical climate during the Last Glacial Maximum. *Geophys Res Lett* 26:1345–1348.
23. Evans MN, Schrag DP (2004) A stable isotope-based approach to tropical dendroclimatology. *Geochim Cosmochim Acta* 68:3295–3305.
24. McCarroll D, Loader NJ (2004) Stable isotopes in tree rings. *Quat Sci Rev* 23:771–801.
25. Barbour MM (2007) Stable oxygen isotope composition of plant tissue: A review. *Funct Plant Biol* 34(2):83–94.
26. Managave SR, et al. (2011) Response of cellulose oxygen isotope values of teak trees in differing monsoon environments to monsoon rainfall. *Dendrochronologia* 29(2): 89–97.
27. Kunert N, Schwendenmann L, Holscher D (2010) Seasonal dynamics of tree sap flux and water use in nine species in Panamanian forest plantations. *Agric For Meteorol* 150:411–419.
28. Brienen RJW, Zuidema PA (2005) Relating tree growth to rainfall in Bolivian rain forests: A test for six species using tree ring analysis. *Oecologia* 146(1):1–12.
29. Kahmen A, et al. (2011) Cellulose (delta)18O is an index of leaf-to-air vapor pressure difference (VPD) in tropical plants. *Proc Natl Acad Sci USA* 108:1981–1986.
30. Williams E, et al. (2005) The drought of the century in the Amazon Basin: An analysis of the regional variation of rainfall in South America in 1926. *Acta Amazon* 35:7.
31. Anchukaitis KJ, Evans MN, Wheelwright NT, Schrag DP (2008) Stable isotope chronology and climate signal calibration in neotropical montane cloud forest trees. *J Geophys Res* 113:G03030.
32. Xu C, Sano M, Nakatsuka T (2011) Tree ring cellulose d18O of *Fokienia hodginsii* in northern Laos: A promising proxy to reconstruct ENSO? *J Geophys Res* 116(D24): D24109.
33. Cruz FW, Jr., et al. (2005) Insolation-driven changes in atmospheric circulation over the past 116,000 years in subtropical Brazil. *Nature* 434(7029):63–66.
34. Vuille M, Bradley RS, Werner M, Healy R, Keimig F (2003) Modeling delta O-18 in precipitation over the tropical Americas: 1. Interannual variability and climatic controls. *J Geophys Res* 108(D6):4175.
35. Baker PA, et al. (2001) The history of South American tropical precipitation for the past 25,000 years. *Science* 291:640–643.
36. Mayle FE, Beerling DJ, Gosling WD, Bush MB (2004) Responses of Amazonian ecosystems to climatic and atmospheric carbon dioxide changes since the last glacial maximum. *Philos Trans R Soc Lond B Biol Sci* 359:499–514.
37. Maslin MA, et al. (2011) Dynamic boundary-monsoon intensity hypothesis: Evidence from the deglacial Amazon River discharge record. *Quat Sci Rev* 30:3823–3833.
38. Yoon JH, Zeng N (2009) An Atlantic influence on Amazon rainfall. *Clim Dyn* 34: 249–264.
39. Labat D, et al. (2004) Wavelet analysis of Amazon hydrological regime variability. *Geophys Res Lett* 31:L02501.
40. Anchukaitis KJ, Evans MN (2010) Tropical cloud forest climate variability and the demise of the Monteverde golden toad. *Proc Natl Acad Sci USA* 107:5036–5040.
41. Poussart PF, Evans MN, Schrag DP (2004) Resolving seasonality in tropical trees: Multi-decade, high-resolution oxygen and carbon isotope records from Indonesia and Thailand. *Earth Planet Sci Lett* 218:301–316.
42. Welp LR, et al. (2011) Interannual variability in the oxygen isotopes of atmospheric CO2 driven by El Niño. *Nature* 477:579–582.
43. Torrence C, Webster PJ (1999) Interdecadal changes in the ENSO-monsoon system. *J Clim* 12:2679–2690.
44. Martinelli LA, Victoria RL, Sternberg LSL, Ribeiro A, Moreira MZ (1996) Using stable isotopes to determine sources of evaporated water to the atmosphere in the Amazon basin. *J Hydrol* 183:191–204.
45. Flanagan LB, Comstock JP, Ehleringer JR (1991) Comparison of modeled and observed environmental influences on the stable oxygen and hydrogen isotope composition of leaf water in *Phaseolus vulgaris* L. *Plant Physiol* 96:588–596.
46. Lettau H, Lettau K, Molion LCB (1979) Amazonias hydrologic cycle and the role of atmospheric recycling in assessing deforestation effects. *Mon Weather Rev* 107: 227–238.
47. Eltahir EAB, Bras RL (1994) Precipitation recycling in the Amazon basin. *Q J R Meteorol Soc* 120:861–880.
48. Thompson LG, et al. (2006) Abrupt tropical climate change: Past and present. *Proc Natl Acad Sci USA* 103:10536–10543.
49. Esper J, et al. (2010) Low-frequency noise in delta C-13 and delta O-18 tree ring data: A case study of *Pinus uncinata* in the Spanish Pyrenees. *Global Biogeochem Cycles* 24: GB4018.
50. Rozanski K, Araguás-Araguás L, Gonfiantini R (1992) Relation between long-term trends of oxygen-18 isotope composition of precipitation and climate. *Science* 258: 981–985.
51. Curtis S, Hastenrath S (1999) Trends of upper-air circulation and water vapour over equatorial South America and adjacent oceans. *Inter J Clim* 19:863–876.
52. Genta JL, Perez-Iribarren G, Mechoso CR (1998) A recent increasing trend in the streamflow of rivers in southeastern South America. *J Clim* 11:2858–2862.
53. Berbery EH, Barros VR (2002) The hydrologic cycle of the La Plata Basin in South America. *J Hydrometeorol* 3:630–645.
54. Andreae MO, et al. (2004) Smoking rain clouds over the Amazon. *Science* 303: 1337–1342.
55. Gedney N, et al. (2006) Detection of a direct carbon dioxide effect in continental river runoff records. *Nature* 439:835–838.
56. Henderson-Sellers A, McGuffie K, Zhang H (2002) Stable isotopes as validation tools for global climate model predictions of the impact of Amazonian deforestation. *J Clim* 15:2664–2677.

Supplemental Information Appendix:

Oxygen isotopes in tree rings are a good proxy for Amazon precipitation and El Niño-Southern Oscillation variability

R.J.W.Brienen[1,2], G.Helle[3], T.L.Pons[4], J-L. Guyot[5], and M. Gloor[1]

[1] Earth and Global Change, School of Geography, University of Leeds, Woodhouse Lane, Leeds LS2 9JT, UK ; [2]Plant Ecology and Biodiversity, Institute of Environmental Biology, Utrecht University, PO Box 80084, 3508 TB Utrecht, the Netherlands; [3] Helmholtz Centre Potsdam, GFZ German Research Centre for Geosciences, Climate Dynamics and Landscape Evolution, Telegrafenberg, 14473 Potsdam, Germany; [4] Plant Ecophysiology, Institute of Environmental Biology, Utrecht University, PO Box 80084, 3508 TB Utrecht, the Netherlands[5]IRD, CP 7091 Lago Sul, 71635–971 Brasilia DF, Brazil

Material and Methods

Study site, species and climate –The vegetation of the study site, Purissima, northern Bolivia (11°24'S, 68 ° 43'W, cf. Fig. 1) can be classified as a tropical lowland moist forest with a canopy height of 25-35 m. high, a basal area of ca. 25 m^2 ha^{-1}, and a stem density of ca. 540 trees per hectare. Total annual precipitation in the study region is 1760 mm, and shows a strong seasonal pattern with a distinct dry season between June and August with a mean monthly precipitation of less than 100 mm per month (cf. Fig. S1b). The influence of ENSO on precipitation in the study site is relative weak (cf. Table S1; low correlations with SST Niño3.4), but ENSO does exhibit a small influence on local temperature.

The study species, *Cedrela odorata* (Meliaceae), is a drought deciduous, relatively light demanding species (1) that loses its leaves during the dry season (between July and September), and forms distinctly visible tree rings marked by a terminal parenchyma band (2). The annual nature of its rings has been proven by several studies using cambial markings (3) and correlations with climate (2, 4), and is induced by cambial dormancy during the dry season (4)

.

Sample collection – Entire stem discs were collected from the bases of ca. 60 logged trees of *Cedrela odorata* (> 60 cm in diameter) with a chainsaw after selective logging in October 2002 from a height between 0.3 and 2.5 meter above the ground. All samples were polished mechanically with sandpaper up to grit 600, and rings were marked and counted in 2-4 radii of each disc and successfully crossdated between trees. Details are described in ref. (2). For this analysis, we selected eight large trees (>60cm) and isolated wood from each individual ring along a single radius using sharp knives and razor blades. Wood was isolated equally from across the entire width of the ring. A few rings were too narrow to isolate sufficient wood material for cellulose extraction. Alpha cellulose was extracted according to (5), and homogenized with an ultasonic device (6). Cellulose samples were weighed and packed into silver capsules, and pyrolized at 1.080°C in an element analyzer (Carlo Erba, Milan, Italy) coupled to an isotope spectrometer (OPTIMA, Micromass Ltd, Manchester, UK). Values are expressed relative to V-SMOW and have an analytic precision of 0.3‰. The eight trees showed a very high degree of synchronization in oxygen isotope ratios with good internal crossdating between trees (Fig. S1; mean inter-tree correlation for 1900-2001= 0.63) and very high "Expressed Population Signal" (EPS; ref. 7) of 0.97, indicating its suitability for palaeoclimatic studies. In all analysis we used the arithmetic mean isotope ratios of the different trees ($\delta^{18}O_{tr}$).

Datasets – Monthly climate data used in this study are from CRU 3.1 climate datasets (precipitation, temperature anomalies, vapour pressure)(8) and from GPCC V5 rain gauge precipitation dataset (9). Data for the local study site came from region 12.5°-10.0°S, 67.5°-70.05°W, and Amazon basin wide data from the area encompassed roughly within 2.5°N to 15.0°S and 50°W to 77.5°W (see main manuscript Fig. 1 for exact boundaries). Monthly data for the Southern Oscillation Index (SOI) are from CRU http://www.cru.uea.ac.uk/cru/data/soi.htm), and all sea surface temperature data from HadISST1 (http://www.metoffice.gov.uk/hadobs/hadisst/). We used the climate explorer (http://climexp.knmi.nl/; (10)) to download all climate data, and to perform correlations between $\delta^{18}O_{tr}$ and spatial fields of Amazon precipitation and SST-anomalies.

Isotope data in precipitation came from the Global Network of Isotopes in Precipitation (GNIP, (11)), accessed through the *Water Isotope System for Data Analysis, Visualization and Electronic Retrieval* (WISER; http://nds121.iaea.org/wiser/index.php). Oxygen isotope data from ice cores of Huascarán and Quelccaya glaciers were obtained from Thompson et al. 2000 (12)http://www.ncdc.noaa.gov/paleo/icecore/trop/) and Sajama net accumulation weighted $\delta^{18}O_{ice}$ records from (13), Fig. 9 in (13)).

Discharge data for Obidos are from HYBAM (ww.ore-hybam.org). Data over the periods 1901 – 1927 and 1947-1968 are reconstructed based on Rio Negro river levels at Manaus and data from other tributaries (14).

Data analysis – All Pearson correlations were performed using SPSS (IBM, SPSS statistics, 19.0.0). To disentangle effects the effects of the oxygen isotope composition of rain water on $\delta^{18}O_{tr}$ from climate effects (cf. Table S2), and disentangle the different climatic effects (i.e., rainfall vs. temperature and vapour pressure, cf. Table S3), we also performed partial correlations. A partial correlation is the relationship between two variables while controlling for a third variable. To do this, the variance from the controlling variable is removed using a linear relationship. So, the partial correlation is the correlation between residuals of a linear regression of each of the two target variables with the controlling variable.

For the calculations of the slopes of the regression between tree ring isotopes ratios ($\delta^{18}O_{tr}$) and isotopes ratios observed in meteoric precipitation ($\delta^{18}O_{prec}$), we used the procedure outlined by ref. (15), explicitly taking errors in both $\delta^{18}O_{prec}$ and the $\delta^{18}O_{tr}$ into account as the magnitude of errors in each of these affects the calculation of the steepness of slopes in a regression (15). Standard (X,Y) regression techniques assume that

all the errors occur in the dependent variable (Y), and these procedure thus minimizes the sum of squares in the Y residuals. However, if there are errors in both variables, which can reasonably well be estimated, the best possible estimate for the slope of the regression is the one that minimizes the sum for both errors. We did this using eq. 7 from York (1966). Errors for $\delta^{18}O_{tr}$ were estimated as the (annual) standard deviation of the different trees included in the analysis. For $\delta^{18}O_{prec}$ for years with lacking monthly $\delta^{18}O$ values, we filled in those lacking months using the monthly means only if data were recorded for at least 4 of the 6 months during the wet season. We estimated the errors in $\delta^{18}O_{prec}$ as the standard deviation of those monthly $\delta^{18}O_{prec}$ records that were filled in using the monthly mean $\delta^{18}O_{prec}$. This least square fitting procedure was programmed using the R statistical platform (16).

To visualize the decadal scale trends in the climate and oxygen isotope date, we used a low-pass, Butterworth filter (17) with a cut-off frequency of 1/5 (removing all variation at 5 yearly time-scales), and an order of 2. We used Matlab v7.8 (The Mathworks) to calculate this low-pass time series.

Calculation of back trajectories –To get a sense of the origin of water vapour at the study site we used the OFFLINE Lagrangian trajectory model (18) to calculate daily kinematic back-trajectories, arriving at 00UT. Trajectory paths were calculated by integration of velocity fields taken from operational analyses of the European Centre for Medium-range Weather Forecasts (ECMWF). The fields at the Lagrangian particle positions are obtained from the analysis fields by cubic Lagrange interpolation in the vertical followed by bilinear interpolation in the horizontal and linear interpolation in time. Trajectories were initialised on a hybrid sigma-pressure coordinate of 0.99, just above the surface. Ten-day back-trajectories were produced, with position output every 6 hours. We produced these trajectories for each day between 1st of October 2001 and 30th of April 2002, thus covering one full rainy season that had a total wet season precipitation close to the long-term average over 1901-2001.

Plant physiological controls – To study till which degree inter-annual variation in $\delta^{18}O$ in *Cedrela* tree rings is influenced by plant physiological controls (e.g., evaporative enrichment of transpiring leaves (19)), we related $\delta^{18}O_{tr}$ to locally recorded climate variables. This showed statistically significant influences of local precipitation, temperature and vapour pressure (Table S2). However, as these correlations may not be due to evaporative enrichment alone, but also to a possible local climate signal in source/soil water ($\delta^{18}O_{prec}$), we statistically removed this source water signal from $\delta^{18}O_{tr}$ using partial correlations. Unfortunately, we do not have data on $\delta^{18}O$ in local precipitation, and thus used instead as proxies isotope records of precipitation in Manaus ($\delta^{18}O_{prec}$) as well as records from the Andean glaciers ($\delta^{18}O_{ice}$ Quelccaya and Huascaran records, ref. 12). $\delta^{18}O_{prec}$ records from Manaus showed better correlations with $\delta^{18}O_{tr}$ and are probably a better measure for $\delta^{18}O_{prec}$ at the study site, but are only very short and discontinuous. In contrast, the Andean glacier records form a continuous, longer record, but may be influenced by additional local (high-altitude) effects. For both records, we used the time window since 1963, as this period has the best spatial coverage of climate stations (cf. Fig. 2 in ref. 20), and as collection of data on meteoric $\delta^{18}O$ started roughly around this period (i.e., most IAEA data for Amazon station start in 1965). Although neither of these records is an optimal measure for the variation in local source water $\delta^{18}O$, the analysis shows that local influences of temperature strongly decrease or disappear (Table S2). Some effect of local precipitation amount and water vapour pressure on $\delta^{18}O_{tr}$ may exist, but controls of both $\delta^{18}O_{prec}$ of Manaus (r=0.86) and of the Andean ice core records (r=0.77) are stronger.

Some additional support for a weak influence of plant physiological controls on inter-annual variation in $\delta^{18}O$ comes from the correlations with local vs. basin-wide variation in climate. As shown in Table S3, basin-wide climate exhibits much stronger correlations, and correlations with local climate disappear nearly completely when controlling for the influence of basin wide wet season precipitation (i.e., when using a partial correlations, see section "Data analysis", cf. last column table S3).

1. Brienen RJW & Zuidema PA (2006) Lifetime growth patterns and ages of Bolivian rain forest trees obtained by tree ring analysis. *J. Ecol.* 94(2):481-493.
2. Brienen RJW & Zuidema PA (2005) Relating tree growth to rainfall in Bolivian rain forests: a test for six species using tree ring analysis. *Oecologia* 146(1):1-12.
3. Worbes M (1999) Annual growth rings, rainfall-dependent growth and long-term growth patterns of tropical trees from the Caparo Forest Reserve in Venezuela. *J. Ecol.* 87(3):391-403.
4. Dunisch O, Bauch J, & Gasparotto L (2002) Formation of increment zones and intraannual growth dynamics in the xylem of *Swietenia macrophylla, Carapa guianensis* , and *Cedrela odorata* (Meliaceae). *IAWA J.* 23(2):101-119.
5. Wieloch T, Helle G, Heinrich I, Voigt M, & Schyma P (2011) A novel device for batch-wise isolation of Î±-cellulose from small-amount wholewood samples. *Dendrochronologia* 29(2):115-117.
6. Laumer W, *et al.* (2009) A novel approach for the homogenization of cellulose to use micro-amounts for stable isotope analyses. *Rapid Commun. Mass Spectrom.* 23(13):1934-1940.
7. Wigley TML, Briffa KR, & Jones PD (1984) On the average value of correlated time series, with applications in dendroclimatology and hydrometeorology. *JApMe* 23(2):201-213.
8. Mitchell TD & Jones PD (2005) An improved method of constructing a database of monthly climate observations and associated high-resolution grids. *IJCli* 25:19.
9. Schneider U, Becker A, Meyer-Christoffer A, ZieseM., & Rudolf B (2011) GPCC Status Report December 2010. (Global Precipitation Climatology Centre (GPCC),), p 13.
10. van Oldenborgh GJ & Burgers G (2005) Searching for decadal variations in ENSO precipitation teleconnections. *Geophys. Res. Lett.* 32(15).
11. IAEA/WMO (2006) Global Network of Isotopes in Precipitation. The GNIP Database.
12. Thompson LG, Mosley-Thompson E, & Henderson KA (2000) Ice-core palaeoclimate records in tropical South America since the Last Glacial Maximum. *JQS* 15(4):377-394.
13. Hardy DR, Vuille M, & Bradley RS (2003) Variability of snow accumulation and isotopic composition on Nevado Sajama, Bolivia. *Journal of Geophysical Research-Atmospheres* 108(D22).
14. Callede J, *et al.* (2004) Evolution of the River Amazon's discharge at Obidos from 1903 to 1999. *Hydrological Sciences Journal-Journal Des Sciences Hydrologiques* 49(1):85-97.
15. York D (1966) Least-squares fitting of a straight line. *Can. J. Phys.* 44(5):1079-1086.
16. R_Development_Core_Team (2011) R: A language and environment for statistical computing, R Foundation for Statistical Computing, URL http://www.R-project.org, Vienna, Austria, 2011.
17. Oppenheim AV & Schafer RW (1989) *Discrete-Time Signal Processing* (Prentice-Hall, Inc., Englewood Cliffs, NJ).
18. Methven J (1997) Offline trajectories: calculation and accuracy. UK Universities Global Atmospheric Modelling Programme. in *Tech. Rep. 44* (University of Reading: Reading, UK).
19. Barbour MM (2007) Stable oxygen isotope composition of plant tissue: a review. *Funct. Plant Biol.* 34(2):83-94.
20. Costa MH, Coe MT, & Guyot JL (2009) Efffects of climatic variability and deforestation on surface water regimes. *Amazonia and Global Change*, (American Geophysical Union), p 576.
21. Yoon JH & Zeng N (2009) An Atlantic influence on Amazon rainfall. *ClDy* 34(2-3):249-264.

Table S1 Pearson correlation coefficients between Sea Surface Temperatures (STT's) in the Niño3.4 region (5°S-5°N, 120°W-170°W) and local and basin wide climate, and Obidos River discharge.

		Period	**Annual**[1]	**Dry** [2]	**Wet**[3]
Basin wide	Precipitation	1901-2001	-0.57***	-0.33***	-0.53***
		1975-2001	-0.65***	-0.33	-0.59***
		1950-1974	-0.48**	-0.44*	-0.45*
		1925-1949	-0.52**	-0.16	-0.49**
		1900-1924	-0.62***	-0.61***	-0.59***
	Temperature	1901-2001	0.54***	0.25*	0.65***
		1975-2001	0.49**	0.19	0.60***
		1950-1974	0.70***	0.42*	0.79***
		1925-1949	0.33	0.05	0.50**
		1900-1924	0.68***	0.37	0.74***
Local	Precipitation	1925-2001	-0.03	0.24*	-0.10
		1975-2001	-0.21	0.41*	-0.33
		1950-1974	0.02	0.07	-0.04
		1925-1949	0.35	0.19	0.45*
	Temperature	1925-2001	0.24	0.13	0.31**
		1975-2001	0.34*	0.22	0.36*
		1950-1974	0.17	0.03	0.33
		1925-1949	-0.02	-0.14	0.12

		Mean	**Max**	**Min**
Obidos River discharge	1902-2001	-0.44***	-0.46***	-0.30**
	1975-2001	-0.64***	-0.53**	-0.44*
	1950-1974	-0.33	-0.35*	-0.34*
	1925-1949	-0.57**	-0.65***	-0.26
	1902-1924	-0.34*	-0.49**	-0.09

***P<0.001, **P<0.01, *P<0.05.
[1] Annual= May to April next year
[2] Dry season= May to September
[3] Wet season= October to April next year

Table S2. Pearson correlation coefficients and *[partial correlations]* between $\delta^{18}O_{tr}$ and (wet season) local and basin wide climate for the period 1963-2001. Wet season was defined as those months with mean precipitation > 100 mm; i.e., October to April next year. Italic values, in brackets, indicate the outcome of partial correlations in which we controlled for the effect of oxygen isotope composition of source water on $\delta^{18}O_{tr}$, using oxygen records from ice cores from Andean glaciers ($\delta^{18}O_{ice}$=mean of Huascaran and Quelccaya, (12)) or isotope records in precipitation from Manaus ($\delta^{18}O_{prec}$ =annual, precipitation weighted $\delta^{18}O$) as proxies for inter-annual variation in source water-$\delta^{18}O$.

	local	*Controlled for*		**basin wide**	*Controlled for*	
		$\delta^{18}O_{ice}$	$\delta^{18}O_{prec}$		$\delta^{18}O_{ice}$	$\delta^{18}O_{prec}$
Precipitation	-0.50**	*[-0.41**	*-0.59*]*	-0.83***	*[-0.79***	*-0.68*]*
Temperature	0.39**	*[0.31*	*0.04]*	0.60***	*[0.59**	*0.37]*
Vapour pressure	0.51**	*[0.42**	*0.43]*	0.44**	*[0.47**	*0.37]*

***P<0.001, **P<0.01, *P<0.05.

Table S3. Pearson correlation coefficients and *[partial correlations]* between $\delta^{18}O_{tr}$ and local and basin wide climate variables for the entire year, dry season, and wet season. Italic values, in brackets, indicate the outcome of partial correlations, in which we controlled for the effect of wet season, basin-wide precipitation.

		Period	**Annual**[1]	**Dry** [2]	**Wet**[3]	**Wet**[3]
Basin wide	Precipitation	1901-2001	-0.50***	-0.16	-0.53***	*[Controlled for effect of rainy season basin wide precipitation]*
		1975-2001	-0.80***	-0.17	-0.85***	
		1950-1974	-0.58**	-0.21	-0.63***	
		1925-1949	-0.12	-0.12	-0.19	
		1901-1924	-0.31	-0.14	-0.33	
	Temperature	1901-2001	0.37**	0.22	0.48**	*[0.26**]*
		1975-2001	0.42*	0.07	0.63***	*[-0.04]*
		1950-1974	0.44*	0.36*	0.47*	*[0.15]*
		1925-1949	0.24	0.43*	0.34	*[0.34]*
		1901-1924	0.28	0.40	0.42*	*[0.25]*
	Vapour pressure	1901-2001	0.36***	0.16	0.42***	*[0.25*]*
		1975-2001	0.35*	0.07	0.46*	*[0.01]*
		1950-1974	0.39*	0.27	0.37*	*[0.09]*
		1925-1949	0.30	0.19	0.42	*[0.38]*
		1901-1924	0.31	0.05	0.42*	*[0.30]*
Local	Precipitation	1925-2001	-0.29**	-0.02	-0.33**	*[0.01]*
		1975-2001	-0.32	0.25	-0.40*	*[0.17]*
		1950-1974	-0.45*	-0.26	-0.45*	*[0.03]*
		1925-1949	0.17	-0.06	0.10	*[0.30]*
	Temperature	1925-2001	0.14	0.11	0.22**	*[0.17]*
		1975-2001	0.29	0.09	0.27	*[-0.04]*
		1950-1974	0.28	0.27	0.26	*[0.2]*
		1925-1949	-0.01	0.01	-0.01	*[0.16]*
	Vapour pressure	1925-2001	0.24*	0.11	0.27***	*[0.19]*
		1975-2001	0.46*	-0.04	0.55**	*[0.07]*
		1950-1974	0.41*	0.37*	0.34	*[0.29]*
		1925-1949	0.07	-0.02	0.14	*[0.26]*

***P<0.001, **P<0.01, *P<0.05.

[1] Annual= May to April next year

[2] Dry season= May to September

[3] Wet season= October to April next year

Table S4 Pearson correlation coefficients between $\delta^{18}O_{tr}$ and Obidos river discharge (ref. 14) for different time periods.

	Mean	Max	Min
1902-2001	-0.58***	-0.61***	-0.25**
1975-2001	-0.80***	-0.81***	-0.46*
1950-1974	-0.72***	-0.83***	-0.28
1925-1949	-0.57**	-0.60***	-0.29
1902-1924	-0.53**	-0.55**	-0.06

***P<0.001, **P<0.01, *P<0.05.

Table S5. Pearson correlation coefficients between $\delta^{18}O_{tr}$ and Southern oscillation Index (SOI) and Sea Surface Temperatures (STT's) in the Niño3.4 region (5°S-5°N, 120°W-170°W) and the tropical north Atlantic (6°N-22°N, 15°-80°W, CRU, HadISST1).

		Annual[1]	Dry [2]	Wet[3]
Southern Oscillation Index	*1901-2001*	-0.50*	-0.31***	-0.52***
	1975-2001	-0.68**	-0.49**	-0.68***
	1950-1974	-0.38*	-0.21	-0.47**
	1925-1949	-0.28	-0.21	-0.24
	1900-1924	-0.47**	-0.20	-0.57**
SST Niño3.4	*1901-2001*	0.50***	0.36***	0.53***
	1975-2001	0.70***	0.57**	0.72***
	1950-1974	0.35*	0.31	0.35*
	1925-1949	0.37*	0.28	0.39*
	1900-1924	0.56**	0.34	0.60***
SST Tropical North Atlantic	*1901-2001*	0.20*	-0.05	0.28*
	1975-2001	-0.02	-0.47**	0.15
	1950-1974	0.01	-0.06	0.01
	1925-1949	-0.09	-0.36*	0.10
	1900-1924	0.47**	0.04	0.59***

***P<0.001, **P<0.01, *P<0.05.

[1] Annual= May to April next year

[2] Dry season= May to September

[3] Wet season= October to April next year

Fig S1. Diagrams of monthly precipitation and oxygen isotopes in precipitation ($\delta^{18}O_{prec}$) for **a)** Manaus (Brazil) and **b)** a composite from the south-western part of the Amazon. Bars indicate monthly precipitation and the lines are the average of $\delta^{18}O$ in meteoric precipitation, obtained from Global Network of Isotopes in Precipitation (ref. 11). The $\delta^{18}O_{prec}$ data for Manaus cover 1965-1990 (not continuous) and the $\delta^{18}O$ data for South-western Amazon are a composite of discontinuous records between 1963 and 1985 from Porto Vehlo and Rio Branco (Brazil), and Rurrenabaque and Trinidad (Bolivia). Precipitation for the south-western Amazon is from nearest climate station, Cobija (Bolivia, 11.0°S, 68.8°W). Error bars are the minimum and maximum values observed.

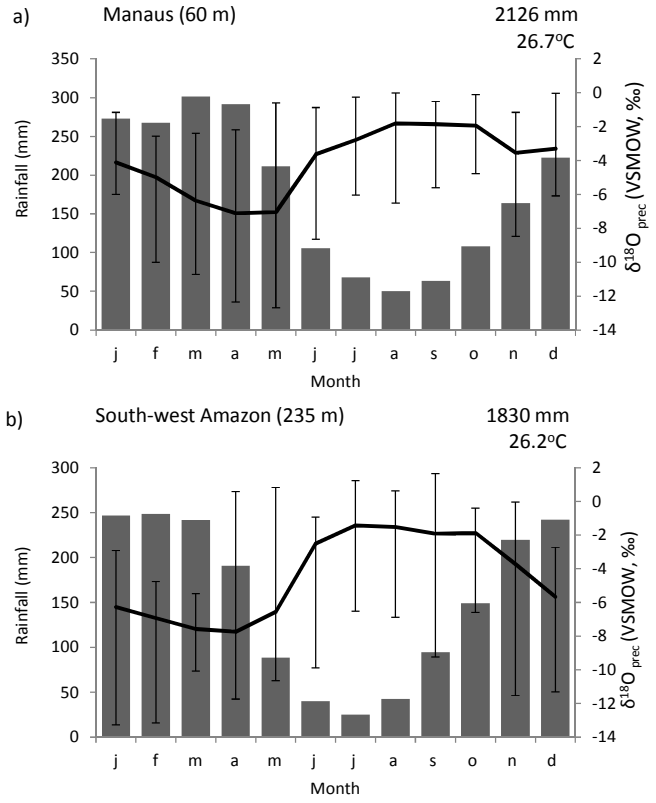

Fig S2. a) Pattern of inter-annual variation in $\delta^{18}O$ in tree ring cellulose in 8 trees *Cedrela odorata*, Bolivia. The mean inter-tree correlation for the period 1900-2001 was 0.63 and the EPS, Expressed Population signal was 0.93, and was calculated according to Wigley et al. (ref. 7). The lower line indicates the number of samples (trees). Note that some years in some trees were not sampled due to lack of sufficient sample materials for extremely narrow rings**. b)** The long-term, mean trend in $\delta^{18}O_{tr}$ for 1863 to 2001. The $\delta^{18}O_{tr}$ series showed a significant increase over time (F=7.47, p=0.007).

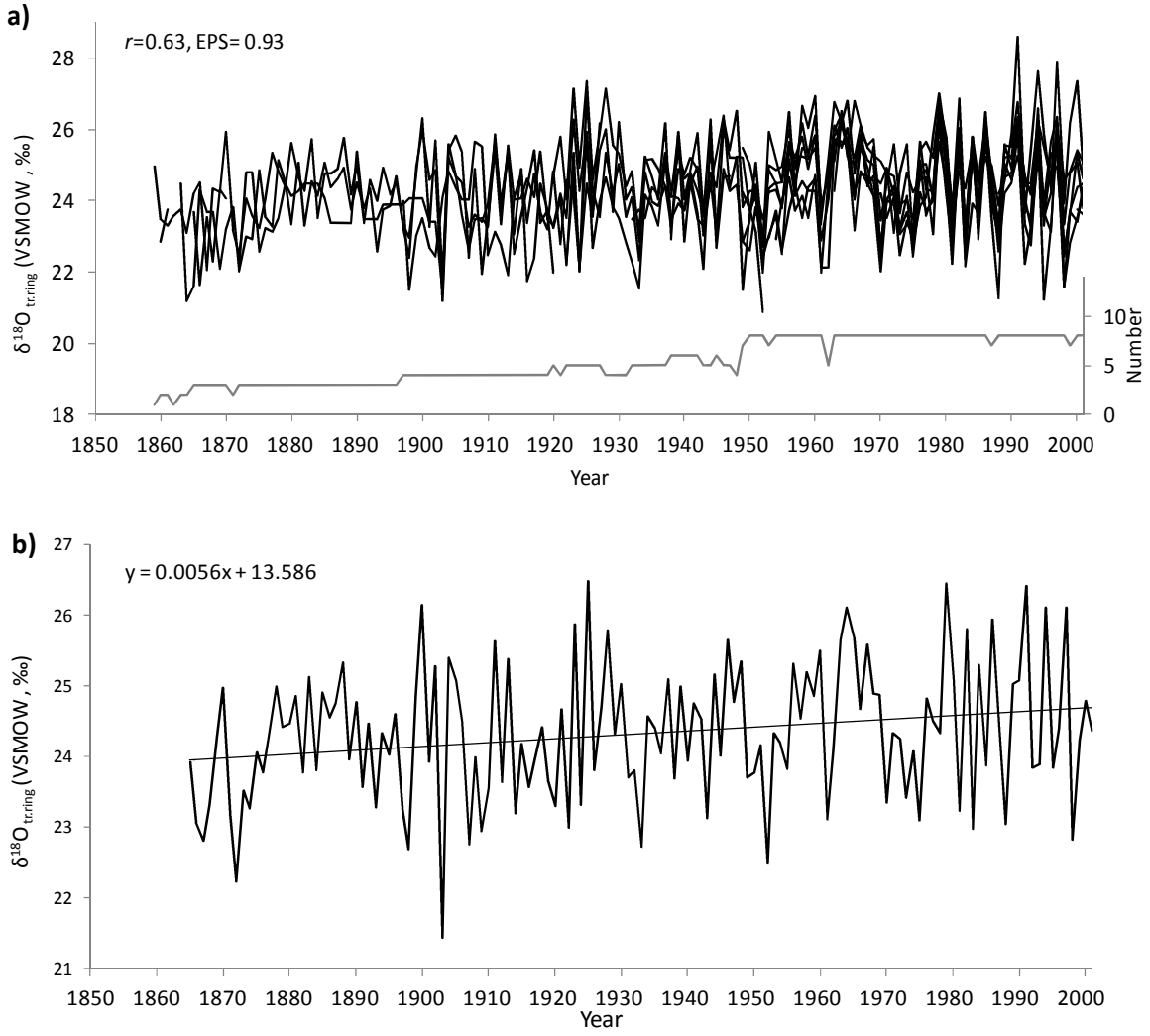

Fig S3. a) Relationship between $\delta^{18}O_{tr}$ and wet season, weighted $\delta^{18}O_{prec}$ from Manaus. Slope of the regression (0.76) was calculated as described in the methods. Oxygen isotope data are from Global Network of Isotopes in Precipitation (11) from the period 1965-1990 (not continuous). **b)** Correlations between weighted $\delta^{18}O_{prec}$from Manaus averaged over a 3-monthly periods and $\delta^{18}O_{tr}$. For example, the correlation coefficient for "*m*" (March) is that of the weighted $\delta^{18}O$ in precipitation during February-April with $\delta^{18}O_{tr}$. Correlations run from previous growing season (March) to the middle of the next dry season (next August). Significant correlations (P<0.05) are indicated by the black bars.

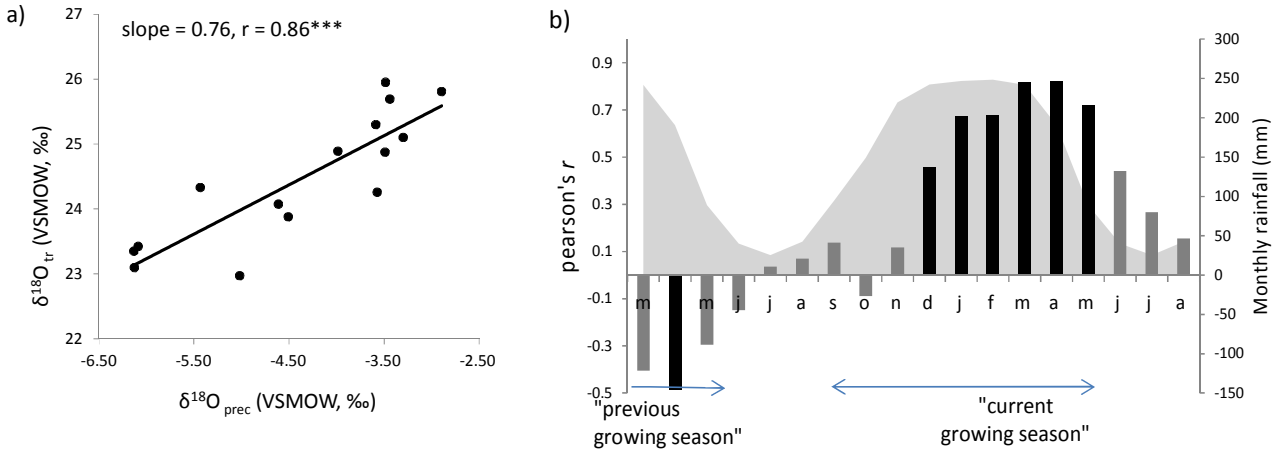

Fig S4. Spatial correlation patterns between $\delta^{18}O_{tr}$ and (gridded) wet season precipitation (from October to March next year, dataset CRU TS 3.1) between 1975-2001. Only correlations P<0.05 are shown (i.e., white grids do not show significant correlations with rainfall). Map was created using the climate explorer (http://climexp.knmi.nl/; ref. (10)). Location of the study site is indicated by the red dot.

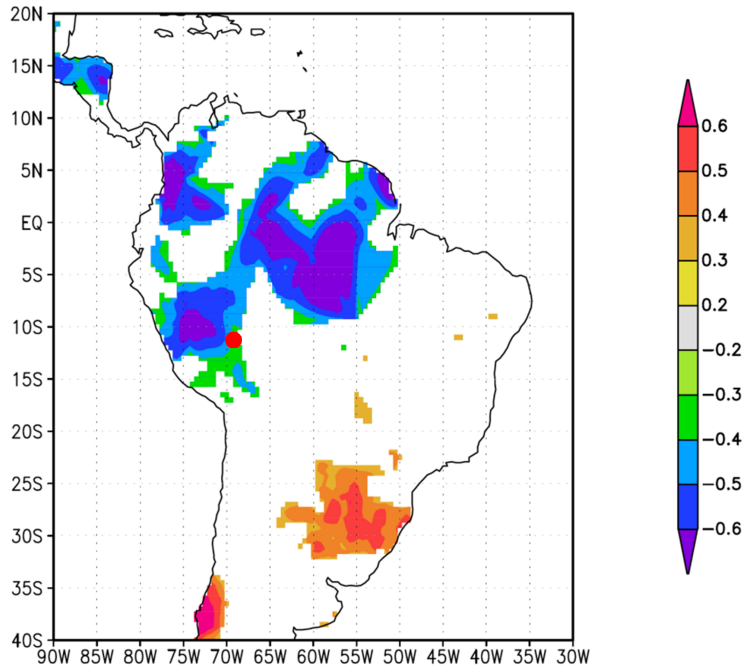

Fig S5. Ten day back-trajectories arriving at the study site (orange dot) during one wet season (i.e., for every day between 1st of October 2001 and 30th of April 2002). See methods for more details.

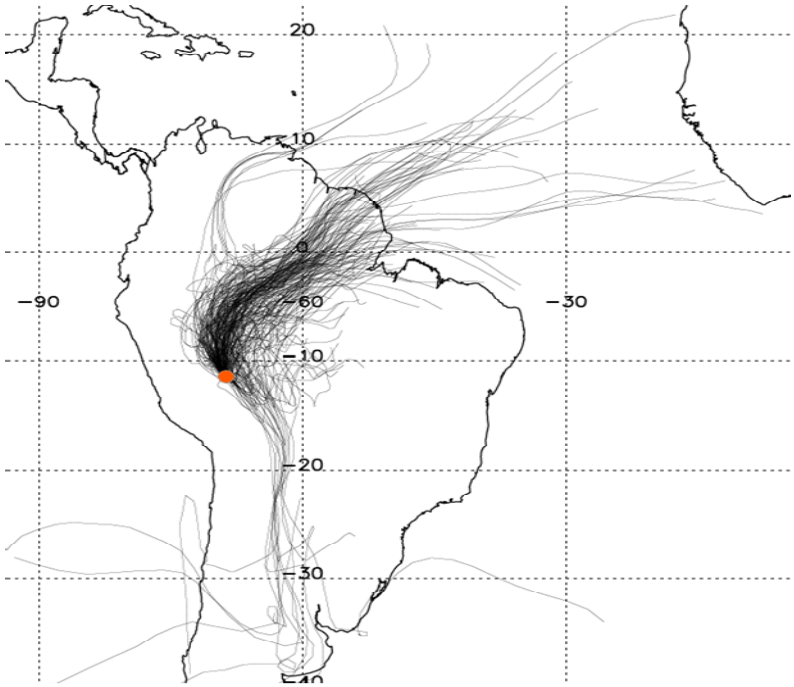

Fig S6. Time series of $\delta^{18}O$ in tree ring cellulose of *Cedrela odorata* (Purissima, Bolivia) and wet season Sea Surface Temperature over the tropical north Atlantic region (6°N-22°N, 15°-80°W, CRU, HadISST1). Boundaries for this region are based on ref. (21). The long-term increase in SST in the tropical north Atlantic is significant (P <0.005).

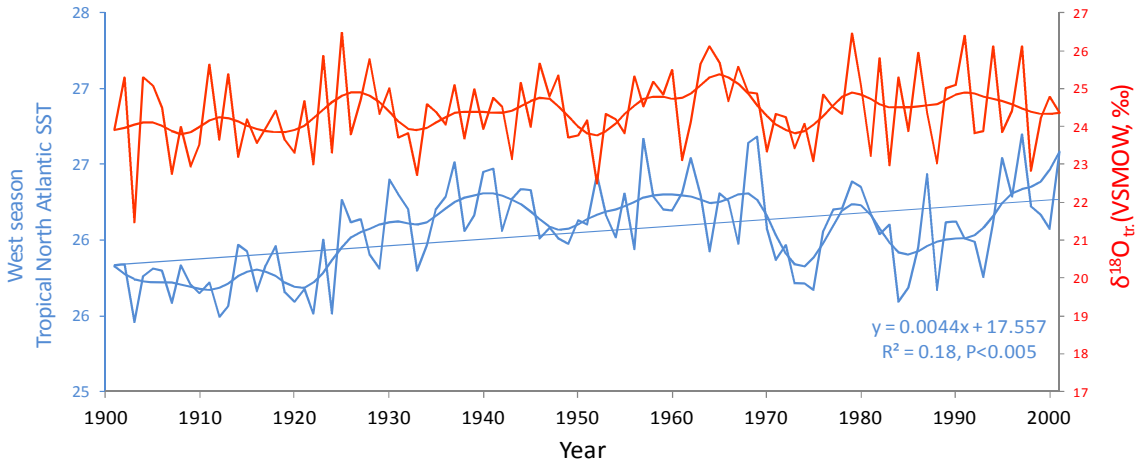

Fig S7. Time series of wet season Amazon precipitation in the CRU data set (8) and GPCC data (9). Only the GPCC dataset showed significant increases over time (F=6.87, P< 0.05).